Asian Journal of Chemistry; Vol. 23, No. 2 (2011), 541-546

ASIAN JOURNAL OF CHEMISTRY

www.asianjournalofchemistry.co.in

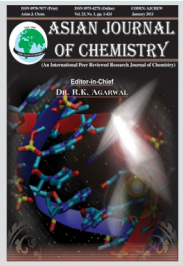

3-Aminopropyltrimethoxysilane Functionalized Mesoporous Materials and Uptake of Metal Ions

ZEID A. ALOTHMAN[1,*] and ALLEN W. APBLETT[2]

[1]Department of Chemistry, College of Science Building # 5, PO Box 2455, King Saud University, Riyadh 11451, Kingdom of Saudi Arabia
[2]Department of Chemistry, Oklahoma State University, 107 Physical Sciences, Stillwater, OK, USA

*Corresponding author: E-mail: zaothman@ksu.edu.sa

(*Received*: 2 February 2010; *Accepted*: 20 September 2010) AJC-9104

γ-Aminopropyl-functionalized mesoporous materials were synthesized by chemical modifcation of a HCl-ethanol washed mesoporous silica (OSU-6-W) with 3-aminopropyltri-methoxysilane (APTMS). The synthesized inorganic-organic hybrids were characterized by solid state ^{29}Si NMR spectroscopy, a titration method and elemental analysis of the modified samples. The average numbers of pendant groups were found to be 2.47 and 4.71 groups/nm^2. Surface area analysis showed that these materials have channel diameters of 43.6 and 36.2 Å and surface areas of 1023 and 709 m^2/g. Infrared spectroscopy, solid state NMR for ^{13}C and ^{29}Si nuclei and X-ray diffraction patterns are in agreement with the success of the preparation of organically-modified mesoporous silicas. Adsorption experiments of Cu^{2+}, Zn^{2+} and Cd^{2+} shows a remarkably high adsorption capacities with an increase in the surface density of amino groups and affected by the pH of the medium, surface areas and pore sizes.

Key Words: Mesoporous silica, Tetraethylorthosilicate, γ-Aminopropyl, Metal ions, NMR.

INTRODUCTION

Saving water to save the planet and to make the future of mankind safe is what we need now. With the growth of mankind, society, science and technology, a considerable amount of industrial waste water is contaminated with heavy metals and radioactive ions. The activities including chemical manufacture, smelting, electroplating, wood treating, industrial and medical use of radioisotopes severely damage the environment by posing risk to wild life and human health[1]. Therefore, improved methods for removing heavy metals or radioactive isotope ions efficiently from contaminated industrial aqueous solutions are highly desired. Existing metal removal methods include standard, conventional techniques such as evaporation, precipitation, electrolytic techniques, membrane separation and fixed and movable bed ion exchange. These methods generally need large and complicated facilities due to various equipment and reagents used in a series of treatments. Adsorption techniques have been reported for the removal of pollutant metal cations using activated carbon[2], polymers[3], zeolites[4,5] and clays[6,7]. The removal of toxic materials is much more difficult because cations comprise similar structure and size, such as sodium, potassium, calcium and magnesium. The adsorptive removal of toxic substances from solution using activated carbon[8,9], zeolites[10] and alumina oxides[11] has also been reported. But these methods are less selective and effective.

The new family of mesoporous molecular sieves M41S[12] and FSM-16[13] with tailorable pore sizes have attracted much attention in the field of catalysis, separation and adsorption. The advantages of ordered silicate mesoporous materials for separation applications include a regular array of uniform pores, controllable pore size and the ability to functionalize the surface for particular separations[10]. But pure siliceous MCM-41 shows limited applications in organic transformations because neutral frame-structure of this material is lack of lacuna, acid sites and acidity[14], which lead to the higher cation-exchange capacities and reactivity[15,16].

Several kinds of surface modification for adsorption of metal ions have been conducted for providing new functions for the surfaces[17,18]. Functionalized mesoporous silica with a high density of amino groups and well-defined mesochannels acquire high capacity and selectivity when applied as adsorbent and separation compound for harmful heavy metal cations, for example cobalt, copper and zinc[19,20]. The large number of primary amino groups with high reactivity enables a variety of chemical modification by immobilizing some ligands with high affinity for specific metal ions onto silica matrices of the mesoporous material. Such modification is expected to further improve the adsorption characteristics of the mesoporous materials[21-23]. Various investigations have been reported on the separation of metals by the use of various kinds of organic materials modified with several chelating ligands, such as

cross-linked polystyrene with ethylenediaminetetraacetic acid (EDTA) and *o*-vanillinsemicarbazone[24] and chitosan with EDTA or DTPA[25].

The purpose of this work is to develop a new family of mesoporous silicas with grafted chelating agents for the removal of pollutant metal ions with increased functional group coverage and pore sizes that were maintained as large as possible. This can be accomplished by using mesoporous silica with large pore size, high surface area and high concentration of hydroxyl (silanol) groups.

EXPERIMENTAL

The chemicals used in this work included: tetraethylorthosilicate (TEOS) as the silica sources and 1-hexadecylamine (HDA) [Aldrich] as the template surfactant and 1,3,5-trimethylbenzene [mesitylene, TCI] as the organic auxiliary reagent. Cyclohexylamine and proton-sponge (1,8-*bis*(dimethylamino)naphthalene) [Aldrich] were used as probe molecules for hydroxyl group determination. Absolute ethyl alcohol [Pharmco, USA], isopropyl alcohol [HPLC-UV Grade, Pharmco, USA], HCl and distilled water were used as solvents. The other chemicals used in this work are 3-aminopropyltrimethoxysilane [$(H_2N(CH_2)_3Si(OCH_3)_3)$ 97.0 %, Aldrich], ethylchloroacetate, toluene 99.8 % HPLC grade, triethylamine (TEA, 99 %, Aldrich), dichloromethane (99.6 %, Aldrich), NaOH (0.025 M). All chemicals were used without further purification.

Solid state ^{13}C NMR was used for the characterization of the ordered mesoporous materials. Solid state ^{13}C CP/MAS NMR spectra were obtained with a Chemagnetics CMX-II solid-state NMR spectrometer operating at 75.694 MHz for carbon-13 and a Chemagnetics 5 mm double resonance magic-angle spinning probe. Carbon-13 cross-polarization/magic-angle spinning (CP/MAS) was carried out with a quasi-adiabatic sequence (1) using two pulse phase modulation (TPPM) decoupling (2) at 50-75 kHz. At least 3600 scans were acquired with a delay of 1.0 s between scans. The MAS samples were collected in a 5.0 mm zirconia rotor spinning at 6.0 kHz, maintained to within a range of ± 5.0 Hz or less with a Chemagnetics speed controller, utilizing a quasi-adiabatic cross-polarization pulse sequence using a 1.0 s pulse delay, a 1.0 ms contact time and a 5.0 μs pulse width. The C-13 CP contact pulse of 1.0 millisecond length was divided into 11 steps of equal length with ascending radiofrequency field strength, while the H-1 contact pulse had constant radio-frequency field strength.

Solid-state ^{29}Si nuclear magnetic resonance (NMR) spectra were recorded on a Chemagnetics CMX-II solid-state NMR spectrometer 5 mm double resonance magic-angle spinning probe operating at resonance frequencies of 59.79 MHz for ^{29}Si nucleus and the chemical shifts are given in ppm from external tetramethylsilane. The ^{29}Si cross-polarization/magnetic-angle spinning (CP/MAS) experiments were 1000-000. The ^{29}Si CP/MAS spectra were acquired in a 5.0 mm zirconia rotor spinning at 6 kHz utilizing a quasi-adiabatic cross-polarizationpulse sequence usinga 5.0 spulse delay, a 9.0 ms contact time, a 7.0 ms pulse width and at least 3000 scans. Proton decoupling was used during acquisition.

The diffuse reflectance infrared Fourier transform (DRIFT) spectra were recorded on a Nicolet Magna 750 FTIR. The spectra were collected for all samples in the range from 4000-400 cm^{-1}. The samples were ground powders diluted with potassium bromide in an approximate ratio of 1:4.

Elemental analysis for C and N was used to measure the amount of functional groups in the samples and was carried out on a LECO TruSpec carbon and nitrogen analyzer. All the adsorption measurements were obtained using a UV-visible spectrophotometer or inductive coupled plasma atomic emission spectroscopy. UV-Visible spectra were recorded on a Perkin Elmer (Lambda EZ 201) spectrometer in the range from 200-800 nm, while the ICP analysis was performed on a Spectro CIROS ICP spectrometer.

Introduction of γ-amino functional groups to the hexagonal mesoporous materials

One step reaction (OSU-6-W-APTMS-1): The activated surfactant free mesoporous silica (TEA-OSU-6-W) was synthesized following the procedure of reported paper[26]. Mesoporous silica-supported γ-aminopropyl functional groups, with 1:1 mole ratio, was prepared by refluxing 3.0 g (*ca.* 50 mmol) of the TEA-OSU-6-W with 50 mmol (9.0 mL) of APTMS in 100 mL of dry toluene in a 250 mL round-bottom flask for 48 h under a dry atmosphere. A drying tube was attached to the reflux apparatus to minimize the influence of moisture. The refluxed mixture was then cooled down to room temperature. The resulting light brown solid was filtered off with a fine filter funnel, washed with toluene three times (3 × 50 mL) and then ethanol, to wash away any excess APTMS. The product became white after the filtration and washing processes. The white solid was then dried at 80 ºC under vacuum for 24 h in an integrated chemical dryer (CHEM-DRY®). The final product weighted 5.04 g (72.2 %) and denoted as OSU-6-W-APTMS-1. IR (KBr, ν_{max}, cm^{-1}): 3737(m), 3604 (m, br), 3357 (s, br), 3297 (s, br), 3016 (s, sh), 2923 (s, sh), 2851 (s, sh), 1862 (w), 1640 (m, sh), 1595 (m, sh), 1542 (m, sh), 1482 (m, sh), 1432 (w), 1361 (m, sh), 1307 (m, sh), 1150 (s, br), 1055 (s, br), 962 (s, sh), 800 (m, sh), 728 (w) and 575 (w).

Three step reaction (OSU-6-W-APTMS-2): In this technique aminopropyl-derivatized mesoporous silica was synthesized in three steps. "One-step reaction" of the above is considered as first step. In the second step, resulting product was placed in a 125 mL Erlenmeyer flask and stirred with 50 mL of distilled water at about 80 ºC for around 5 h in order to hydrolyze the methoxy groups. After cooling to room temperature, the sample was centrifuged down to recover the solid product, the water was decanted off and the mesoporous silica was dried at 80 ºC under vacuum for 24 h. In the third step, the hydrated mesoporous silica was then suspended in 100 mL of dried toluene in a 250 mL round-bottom flask, treated with 25 mmol (*ca.* 4.5 mL) of APTMS and taken to reflux for 48 h under a dry atmosphere. After cooling to room temperature, the reaction mixture (light brown) was filtered with a fine filter funnel. The solid was washed copiously with toluene (3 × 50 mL) and then ethanol, to rinse away any excess APTMS then dried at 80 ºC under vacuum for 24 h. The final white product was 5.73 g and designated as OSU-6-W-

APTMS-2. The filtrates from the first and third steps were collected and 30 mL of the total filtrate mixture was reserved for the functional group concentration determination. IR (KBr, ν_{max}, cm^{-1}) of the main product: 3359 (s, sh), 3302 (s, sh), 2920 (s, sh), 2850 (s, sh), 1873 (w), 1638 (m), 1600 (m, sh), 1535 (s, sh), 1467 (s, sh), 1408 (m), 1392 (m, sh), 1236 (s, br), 1188 (s, br), 1062 (s, br), 993 (m, br), 795 (m, sh) and 721 (m, sh).

Metal uptake experiments: The adsorption and separation experiments were conducted by shaking five different amounts (25, 50, 75, 100 and 125 mg) of the amino-functionalized mesoporous silica systems, OSU-6-W-APTMS-(1 and 2), each in a different glass vial for 4 h with 10 mL of 100 ppm of aqueous solution of the appropriate metal(II) nitrate ions (Cu^{2+}, Zn^{2+} and Cd^{2+}). Measurement of the metal ion concentration was carried out by allowing the insoluble complex to settle down, withdrawing an appropriate volume of the supernatant using a micropipette and then filtrating using a 0.45 μm membrane syringe. The metal ion uptake was calculated as mmol of M^{2+}/g ligand. A linear range of the calibration curve for each metal was used in order to calculate the unknown concentration.

RESULTS AND DISCUSSION

The new grafting procedure used herein utilized conditions whereby hydrolysis of the silicon alkoxides during the grafting procedure was avoided as much as possible by maintaining a strictly dry atmosphere during the silanization step. This prevented polymerization of the silyl reagent *via* formation of silicon-oxygen linkages and promoted the maximum coverage of the surface with the immobilized 3-aminopropyltrimethoxysilane functional groups. After silanization, the remaining alkoxides groups on silica were removed by hydrolysis during water wash causing a concomitant condensation reaction between adjacent grafted silyl groups that creates an Ormosil polymer grafted to the mesoporous silica surface. Following this procedure with a second silanization step enhances the maximum surface density of silanes by at least 30 %[27].

Characterization of textural properties

X-Ray diffraction measurements: The X-ray diffraction patterns in the range of 1.0-8.0º of OSU-6-W and the two functionalized samples, OSU-6-W-APTMS-1 and OSU-6-W-APTMS-2, are shown in Fig. 1. The XRD patterns of the samples show strong (100) peaks and proportional (110) and (200) peak intensities, confirming the presence of the hexagonal structures without affecting the framework integrity of the ordered mesoporous OSU-6-W[12,28]. It is also to be noted that the (100) peak gradually shifts to higher angles with increasing the amount of functional group on the surface from OSU-6-W-APTMS-1 to OSU-6-W-APTMS-2. The increase in wall thickness (Table-1) with functionalization would correspond to an extra layer of Si-O-Si homogeneously spread on the original wall. The broadening of d_{100} peak with the increase in the loading of the functional groups, indicating a slight alteration of the ordering of the mesoporous structure and more functional groups on the surface.

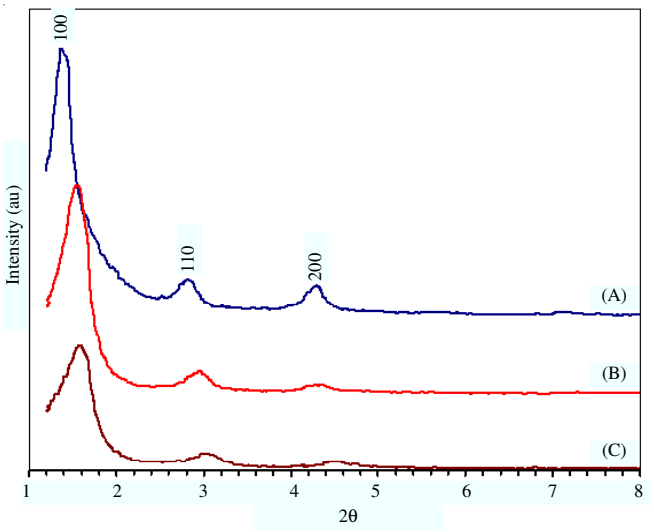

Fig. 1. XRD patterns in the range of 1.0-10.0º of; (A) pristine HCl-ethanol washed ordered mesoporous material, OSU-6-W and the functionalized OSU-6-W with 3-aminopropyltrimethoxysilane: (B) OSU-6-W-APTMS-1 and (C) OSU-6-W-APTMS-2. The spectra are shifted vertically for the sake of clarity

TABLE-1
TEXTURAL PROPERTIES DETERMINED FROM NITROGEN ADSORPTION-DESORPTION EXPERIMENTS AT 77 K AND POWDER XRD MEASUREMENTS

Sample	Specific surface area (m^2/g)	Total pore volume (cm^3/g)	Average pore size (Å)	d_{100} (Å)	Wall thickness (Å)
OSU-6-W	1283	1.24	51.1	62.4	20.9
OSU-6-W-APTMS-1	1023	0.98	43.6	57.7	23.0
OSU-6-W-APTMS-2	709	0.66	36.2	55.4	27.8

Identification of functional groups

Solid state ^{29}Si CP/MAS NMR spectroscopy: Solid state ^{29}Si CP/MAS NMR is a sensitive and reliable technique for qualitative and quantitative determination of both Si-OH groups on solid surfaces and the total loading of the functional groups on the silica surfaces[14,28]. Multipeak curve fitting indicates that for sample OSU-6-W, three peaks can be identified in the vicinity of -100 ppm. According to Sindorf *et al.*[29], a low intensity peak at -91.2 ppm corresponds to surface silicon atoms with two siloxane bonds and two *geminal* silanol groups either single or hydrogen-bonded, represented as $(SiO)_2{\cdot}Si(OH)_2$ and labeled as a Q^2 silicon in Fig. 2(A). A peak at -100.4 ppm attributed to surface silicon atoms with three siloxane bonds and one (isolated) silanol group, represented as $(SiO)_3{\cdot}Si\text{-}OH$ and labeled as a Q^3 silicon. A resonance at -107.9 ppm attributed to surface silicon atoms with four siloxane bonds, *i.e.*, $(SiO)_4{\cdot}Si$ and labeled as a Q^4 silicon. The two amino functionalized samples, Fig. 2 (B) and (C), show two peaks that are located near -100 and -110 ppm, corresponding to Q^3 and Q^4 silicon environments. Additionally, the OSU-6-W-APTMS-1 sample has another three peaks at -51.9, -59.3 and -67.1 ppm corresponding to T^1, T^2 and T^3 silicon environments and OSU-6-W-APTMS-2 sample has another two peaks at -57.3 (T^2) and -66.6 ppm (T^3). By comparison between the two modified samples, the intensity of the peak

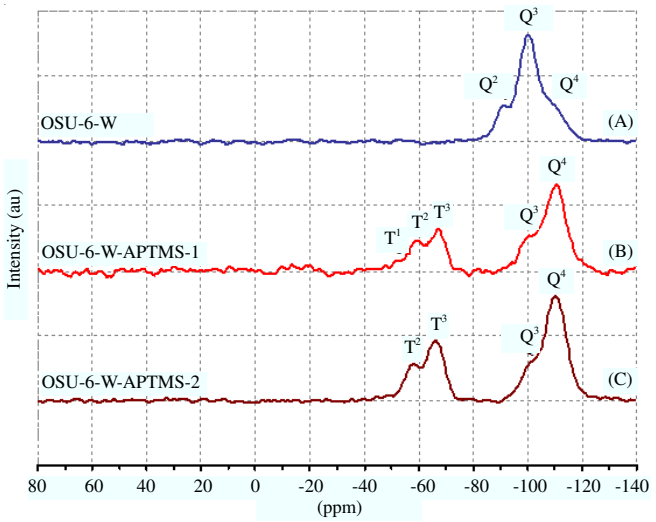

Fig. 2. ^{29}Si CP/MAS NMR spectra of; (A) HCl-Ethanol washed mesoporous silica, OSU-6-W, (B) the modified OSU-6-W-APTMS-1 and (C) the modified OSU-6-W-APTMS-2

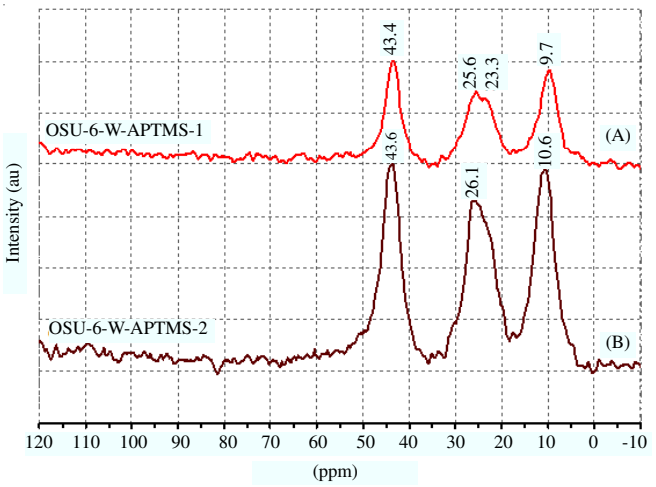

Fig. 3. Solid state ^{13}C CP/MAS NMR spectra of the modified samples with amine groups, (A) OSU-6-W-APTMS-1 and (B) OSU-6-W-APTMS-2

at around -100 ppm is smallest for OSU-6-W-APTMS-2 sample providing evidence of greater functionalization of this sample.

The three resonances for OSU-6-W-APTMS-1 can be assigned as the following: (i) the resonance at *ca*. -51.9 ppm arises from isolated SiO_3 groups that are not bound to any neighboring siloxanes, (ii) the resonance at *ca*. -59.3 ppm arises from terminal groups that are only bound to one neighboring siloxane and (iii) the resonance at *ca*. -67.1 ppm arises from cross-linked groups that are bound to two neighboring siloxanes. The two resonances for OSU-6-W-APTMS-2 can be assigned as follows: (i) at *ca*. -57.3 ppm arises from terminal groups that are only bound to one neighboring siloxane and (ii) at *ca*. -66.6 ppm arises from cross-linked groups that are bound to two neighboring siloxanes. The dominant peak in the OSU-6-W-APTMS-1 and OSU-6-W-APTMS-2 spectra is attributed to the cross-linked siloxane group. The surface coverage of the functionalized monolayer of OSU-6-W is estimated to be greater in the OSU-6-W-APTMS-2 sample than in the OSU-6-W-APTMS-1 sample. This conclusion is based on the higher intensity of the peak for T^3 of OSU-6-W-APTMS-2. Also, the absence of the peak for T^1 in the spectrum of OSU-6-W-APTMS-2 is evidence for higher loading and greater homogeneity of the functional groups on the surface. OSU-6-W-APTMS-1 has peaks with intensities that are more than approximately 50 % while the OSU-6-W-APTMS-2 are higher than 75 % surface coverage of the sample previously reported[18].

Solid state ^{13}C CP/MAS NMR spectroscopy: The presence of covalently linked organic moieties bearing amine groups in the derivitized OSU-6-W mesoporous silicas was also confirmed by the solid state ^{13}C CP/MAS NMR spectroscopy[15,16]. Fig. 3(A) shows resonances for the OSU-6-W-APTMS-1 sample, whereas, Fig. 3(B) shows resonances related to the OSU-6-W-APTMS-2 sample. These data confirmed that the γ-aminopropyl groups were not damaged by either functionalization method. Peaks corresponding to the organosiloxane moieties are relatively broad, indicating restricted mobility of the functional groups attached to the siloxane framework. The presence of a small peak at around 23.3 ppm indicates the presence of a small amount of methoxy groups, which in turn confirms the low loading of the functional groups in the OSU-6-W-APTMS-1 sample. The low intensity of the peaks of OSU-6-W-APTMS-1 compared to OSU-6-W-APTMS-2 also reflects lower surface loading from the one-step method.

Alternating silanization and washing in water enhances the maximum surface density of silanes by at least 30 %[30]. The amines catalyze reactions between methoxysilanes and hydroxyl groups on silica[31] suggest that aminomethoxysilanes would immobilize on silica more efficiently than methoxysilanes. The ability to form a pseudo-five-membered ring in γ-aminosilanes[32], offers a possibility for self-catalytic reaction enhancement for the APTMS aminosilanes[31].

Fourier transform infrared spectroscopy (FT-IR): Fig. 4 shows the FT-IR spectra of the two modified samples along with the unmodified mesoporous OSU-6-W. The O-H bond stretching bands of silanol groups were observed at 3200-3800 cm^{-1}. Silanol groups on the silica surface of OSU-6-W exist as several types, such as isolated, hydrogen bonded and geminal types of silanol[33]. The IR absorption bands of these silanol groups correspond to the peaks at 3740, 3200-3600 and 3715 cm^{-1}, respectively. For OSU-6-W, the concentration of surface silanol groups was calculated to be 14.43 mmol/g (6.77 molecule/nm^2).

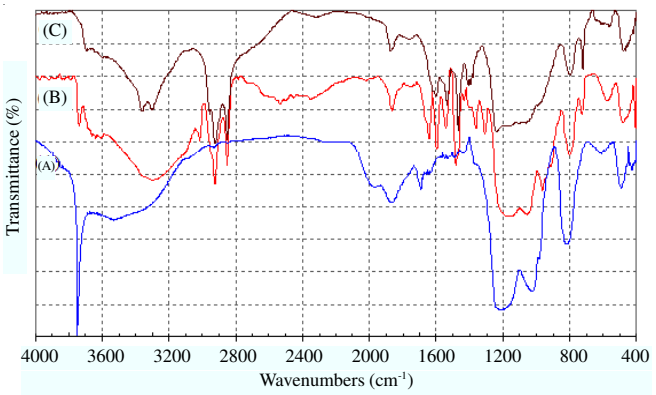

Fig. 4. Fourier transform-infrared spectroscopy (FT-IR) of OSU-6-W (A), OSU-6-W-APTMS-1 (B) and OSU-6-W-APTMS-2 (C)

Total surface loading of OSU-6-W with APTMS: The degree of silylation was evaluated using the ^{29}Si CP/MAS NMR spectrum[34]. The Q^2, Q^3 and Q^4 of OSU-6-W are found at -91.2, -100.4 and -107.9 ppm, respectively, Fig. 2(A). The silicon atom of the silylating agent APTMS is seen at -51.9, -59.3, -67.1, -92.6, -100.5 and -110.3 ppm for OSU-6-W-APTMS-1 sample and at -57.3, -66.6, -100.6 and -110.3 ppm for OSU-6-W-APTMS-2 sample, Fig. 2(B and C). The relative peak areas of the spectra are given in Table-2. From these data, the silanol concentration [SiOH] and the degree of silylation [APTMS] per gram of dry OSU-6-W (mol/g) can be obtained from the formula:

$$[SiOH] = [(I_Q^3 + 2 \times I_Q^2)/(60 \times I_Q^4 + 69 \times I_Q^3 + 78 \times I_Q^2)]$$
$$[APTMS] = [(IAPTMS)/(60 \times I_Q^4 + 69 \times I_Q^3 + 78 \times I_Q^2)]$$

I_i represents the line intensity of the various silicon lines in the ^{29}Si MAS NMR spectrum. The denominator of both equations relates to the chemical composition of the dry OSU-6-W sample. The ^{29}Si CP/MAS NMR signal areas are therefore multiplied by the respective molecular weight of Q^4, Q^3 and Q^2. The nominator weighs the I_i lines relative to the dry OSU-6-W.

A significantly large coverage of functional groups 4.71 molecule/nm^2 was obtained compared[35] with the reported 2.53 molecule/nm^2. In the presence of water, the aminosilane molecules are attached beyond the density of isolated silanols (total silanol concentration including isolated and geminal is 6.77 OH groups/nm^2). So the total coverage is controlled by the specific surface area and pore size of the silica, rather than the hydroxyl group content.

Uptake capacities of Cu^{2+}, Zn^{2+} and Cd^{2+}: The uptake capacities of the mesoporous silicas with immobilized monoamine ligand systems were investigated using different amount of the absorbents, OSU-6-W-APTMS-(1 and 2) and one constant concentration of copper, zinc and cadmium ions (100 ppm) at pH 5.5, 6.0 and 7.0, respectively[35]. The results are shown in Figs. 5(a) and 5(b). The tendency of these divalent metal ions to chemisorb to the monoamine ligand system at the optimum conditions increases in the order: $Cd^{2+} < Zn^{2+} < Cu^{2+}$. For both functionalized samples, it is shown that the uptake of all metal increases with an increase of the amount of absorbent. Moreover, the uptake capacities increase with the increasing of the total coverage of the surface with the functional groups from OSU-6-W-APTMS-1 to OSU-6-W-APTMS-2. The maximum uptakes were calculated from the Langmuir adsorption isotherms. The uptake capacities are listed in Table-3. The uptake capacities of the OSU-6-W-APTMS-1, Fig. 5(a), are correlated to the approximate formation of 2 Cd^{2+}:3 NH_2, an approximate 1 Zn^{2+}:1 NH_2 and 1 Cu^{2+}:1 NH_2 complexes. The absorption of greater than one copper ion per amine may be due to inclusion of anionic copper nitrate complexes as counterions. In the case of OSU-6-W-APTMS-2, Fig. 5(b), the stoichiometry of uptake per amine group changed. The cadmium uptake corresponded to formation of 1 Cd^{2+}:2 NH_2 complex. The uptake of zinc exceeded this to give a ratio of Zn^{2+}:NH_2 of 1:1.3 which is likely a mixture of 1:1 and 1:2 complexes. Again, the number of copper ions exceeded the number of amine groups with a ration of 1 Cu^{2+}:1 NH_2.

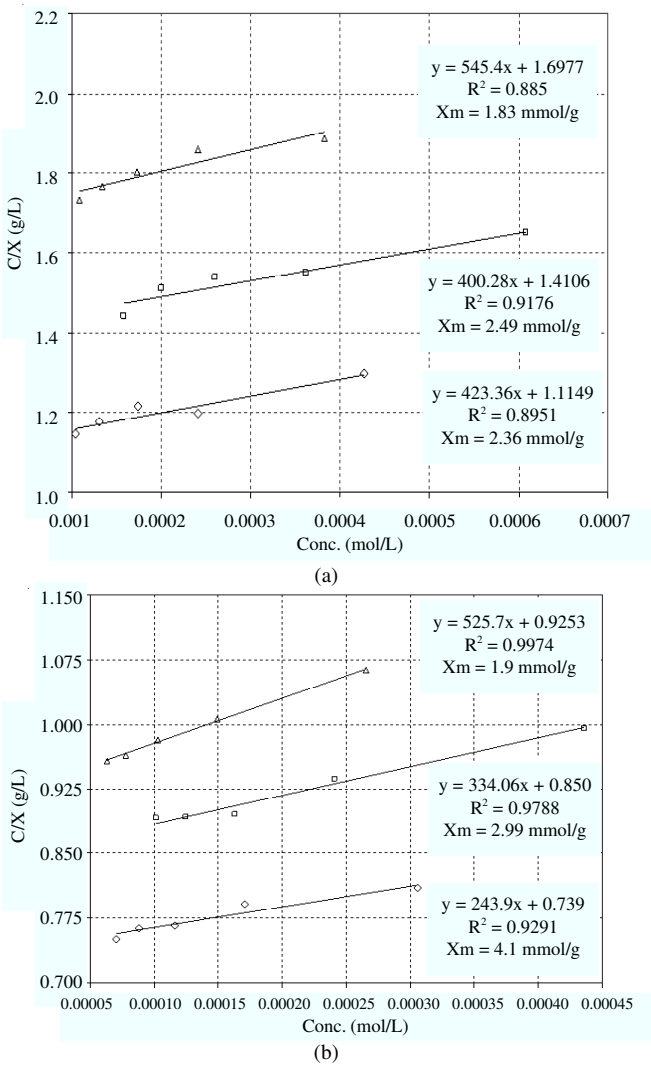

Fig. 5. Langmuir adsorption isotherms of (◊) Cu^{2+}, (□) Zn^{2+} and (△) Cd^{2+} ions adsorbed by absorbent (a) OSU-6-W-APTMS-1 and (b) OSU-6-W-APTMS-2

TABLE-3
THE UPTAKE CAPACITIES FROM THE LANGMUIR ADSORPTION ISOTHERMS

Adsorbent	Uptake capacity (mg/g)		
	Cu^{2+}	Zn^{2+}	Cd^{2+}
OSU-6-W-APTMS-1	149.9	162.9	205.7
OSU-6-W-APTMS-2	260.6	195.6	213.6

TABLE-2
SOLID STATE ^{29}Si CP/MAS NMR DECONVOLUTION RESULTS

Sample	Q^4 (%)	Q^3 (%)	Q^2 (%)	[SiOH] (mmol/g)	[SiOH] (molecule/nm^2)	[APTMS] (group/nm^2)
OSU-6-W	14.38	71.73	13.89	14.43	6.77	–
OSU-6-W-APTMS-1	60.84	31.44	7.72	7.29	4.30	2.47
OSU-6-W-APTMS-2	82.98	17.01	0	2.76	2.06	4.71

Adsorbent regeneration: The adsorbent was regenerated for further metal ion uptake by treatment of the copper loaded material with an aqueous solution of 2.0 M HCl. The regenerated material showed a high metal ion uptake capacity of 95 % of the original material which is better than reported acid-regenerated P-$(CH_2)_3NH_2$[35]. This suggests that the synthesized materials have high stabilities toward acid leaching of the functional groups. These amino-functionalized materials show higher metal ion uptake than the aminosilyl derivitized materials prepared by El-Nahhal *et al.*[36].

Conclusion

The improved technique allows surface concentration of amino-functional groups of around 4.71 group/nm^2, almost 1.6 times higher than what is possible without water treatment[30]. However, the reaction conditions and the silanol group concentration play an important role in determine the amount of the functional groups. The use of water in an intermediate step, to hydrolyzed methoxy group left after first functionalization step, showed an improvement in the total surface coverage. The combination of two synthesis procedures was used to yield a highly thiol-functionalized mesostructure which retained channels with mesopore-range dimensions (diameters > 30 Å). The presented work may also prove to be more cost-effective than that used to prepare FMMS because it allows the recovery of the expensive assembly surfactant, requires fewer preparative steps and reagents and is accomplished in a shorter time. The inorganic-organic hybrid, OSU-6-W-GPTMS-2 had a very high Cu(II), Zn(II) and Cd(II) ion adsorption and showed good regeneration ability. Beyond their applications in environmental cleanup, OSU-6-W-APTMS-(1 and 2) provide unique opportunity to introduce molecular binding sites and to rationally design the surface properties (for example, wettability and charge density distribution) of mesoporous materials. Specific groups in the functionalized monolayers can be used to attach new functional groups or to stimulate mineral deposition[37,38].

ACKNOWLEDGEMENTS

The authors gratefully acknowledged the financial support from Oklahoma State University and King Saud University for this research work.

REFERENCES

1. S.D. Faust and O.M. Ali, Chemistry of Water Treatment, Butterworth & Co. Publ. Ltd., Boston (1983).
2. D. Mohan, V.K. Gupta, S.K. Srivastava and S. Chander, *Colloids Surf. A*, **177**, 169 (2001).
3. R.R. Navarro, K. Sumi and M. Matumura, *Water Res*., **33**, 2037 (1999).
4. C.P. Huang and O.J Hao, *J. Environ. Tech. Lett*., **10**, 863 (1989).
5. M.J. Zamzow, B.R. Eichbaum, K.R. Sandgren and D.E. Shanks, *Seper. Sci. Tech.*, **25**, 1555 (1990).
6. L. Mercier and T.J. Pinnavaia, *Micropor. Mesopor. Mater*., **20**, 101 (1998).
7. R. Celis and M.C. Hermosin, *J. Environ. Sci. Tech*., **34**, 4593 (2000).
8. S.K. Gupta and K.Y. Chen, *J. Water Pollu. Control Fed*., **50**, 493 (1978).
9. C.P. Huang and P.L.K. Fu, *J. Water Pollu. Control Fed*., **56**, 233 (1984).
10. G.M. Haggerty and R.S. Bowman, *Environ. Sci. Tech*., **28**, 452 (1994).
11. C.H. Wu, C.Y. Kuo, C.F. Lin and S.L. Lo, *Chemosphere*, **47**, 283 (2002).
12. J.S. Beck, J.C. Vartuli, W.J. Roth, M.E. Leonowicz, C.T. Kresge, K.D. Schmitt, C.T.W. Chu, D.H. Olson, E.W. Sheppard, S.B. McCullen, J.B. Higgins and J.L. Schlenker, *J. Am. Chem. Soc*., **114**, 10834 (1992).
13. S. Inagaki, Y. Fukushima and K. Kuroda, *J. Chem. Soc. Chem. Commun*., 680 (1993).
14. J. Xu, W. Chu and S. Luo, *J. Mole. Catal. A: Chem*., **256**, 48 (2006).
15. R.F. Howe, *Appl. Catal. A Gen*., **271**, 3 (2004).
16. M. Stocker, *Micropor. Mesopor. Mater*., **82**, 257 (2005).
17. K.F. Lam, K.L. Yeung and G. McKay, *Environ. Sci. Tech*., **41**, 3329 (2007).
18. K.F. Lam, K.L. Yeung and G. McKay, *Micropor. Mesopor. Mater*., **100**, 191 (2007).
19. X. Feng, G.E. Fryxell, L.Q. Wang, A.Y. Kim, J. Liu and K.M. Kemner, *Science*, **276**, 923 (1997).
20. V. Antochshuk and M. Kemner, *Chem. Commun*., 258 (2002).
21. T.S. Zemanian, G.E. Fryxell, J. Liu, S. Mattigod, J.A. Franz and Z. Nie, *Langmuir*, **17**, 8172 (2001).
22. K. Kruk, T. Asefa, M. Jaroniec and G.A. Ozin, *J. Am. Chem. Soc*., **124**, 6383 (2002).
23. L. Beaudet, K.Z. Hossain and L. Mercier, *Mater*., **15**, 327 (2003).
24. V.K. Jain, A. Handa, S.S. Sait, P. Shrivastav and Y.K. Agrawal, *Anal. Chim. Acta*, **429**, 237 (2001).
25. K. Inoue, K. Yoshizuka and K. Ohto, *Anal. Chim. Acta*, **388**, 209 (1999).
26. Z.A. AlOthman and A.W. Apblett, *Chem. Eng. J*., **155**, 916 (2009).
27. A.V. Krasnoslobodtsev and S.N. Smirnov, *Langmuir*, **18**, 3181 (2002).
28. D.J. Macquarrie, *Chem. Commun*., 1961 (1996).
29. D.W. Sindorf and G.E. Maciel, *J. Phys. Chem*., **86**, 5208 (1982).
30. A.V. Krasnoslobodtsev and S.N. Smirnov, *Langmuir*, **18**, 3181 (2002).
31. L.D. White and C.P. Tripp, *J. Colloid Interf. Sci*., **227**, 237 (2000).
32. J.P. Blitz, R.S. Murthy and D.E. Leyden, *J. Colloid Interf. Sci*., **126**, 387 (1988).
33. X.S. Zhao, G.Q. Lu, A.J. Whittaker and G.J. Millar and H.Y. Zhu, *J. Phys. Chem. B*, **101**, 6525 (1997).
34. B.H. Wouters, T. Chen, M. Dewilde and P.J. Grobet, *Micropor. Mesopor. Mater*., **44-45**, 453 (2001).
35. D.J. Macquarrie, D.B. Jackson, J.E.G. Mdoe and J.H. Clark, *New J. Chem*., **23**, 539 (1999).
36. I.M. El-Nahhal, F.R. Zaggout and N.M. El-Ashgar, *Anal. Lett*., **33**, 2031 (2000).
37. D.J. Macquarrie, M. Rocchia, B. Onida, E. Garrone, P. Lentz, J.B. Nagy, D. Brunel, A.C. Blanc and F. Fajula, *Stud. Surf. Sci. Catal*., **135**, 4849 (2001).
38. D. Brunel, A.C. Blanc, E. Garrone, B. Onida, M. Rocchia, J.B. Nagy and D.J. Macquarrie, *Stud. Surf. Sci. Catal*., **142B**, 1395 (2002).